DYNAMIC SELECTION OF PHYSICAL CHANNELS FOR ADAPTIVE IMPROVEMENT OF LINK QUALITY USING AN AGILE APERTURE ANTENNA

R. S. Westafer*, E. J. Strates, M. G. Habib, B. N. Baker
Advanced Concepts Laboratory, Georgia Tech Research Institute,
400 Tenth St NW, Atlanta, GA, USA 30332-0866

This paper describes integration of a software defined antenna (SDA) and a software defined radio (SDR) to enable dynamic and automatic selection of physical propagation channels. The SDA, an agile aperture antenna (A3), provides monolithic microdiversity, i.e. multiple antenna states within a single structure and within a space having maximum dimension of approximately one wavelength. In this way physical channel selection occurs outside, and therefore augmenting, the front-end electronics. The independent controllable parameters for channel access include: frequency, polarization (full Poincaré sphere), and pattern (in two dimensions). Several different tests were conducted to maximize a quality figure of merit calculated by the radio. Both library-based and evolutionary search techniques were used, resulting in short term channel improvements on the order of 10 dB, and long term fully optimized improvements on the order of 20 dB.

1. INTRODUCTION

The electromagnetic environment can be mapped and computed with increasing accuracy, enabling improved predictive models of link capacity [1-3]. However, changes to the environment and unknown or inaccurately known dynamics, e.g. vehicle motion, could render the models ineffective. Therefore, an adaptive approach is advantageous, enabling selection of the best available propagation channel, given whatever information is available, possibly only a single scalar figure of merit (FoM) calculated by a radio. Multi-input multi-output (MIMO) solutions are suited to such problems, but they are often accompanied by an increase in power required to receive and combine several RF signals simultaneously. In contrast, this paper describes the application of a single reconfigurable antenna to select propagation channels at the physical layer, a channelization method that requires only one radio receiver, and that exercises control over degrees of freedom not possible in a front end, e.g. polarization. Such integration of reconfigurable antennas with radios and digital signal processing has long been lacking, an observation noted as early as 2003 [4].

*ryan.westafer@gtri.gatech.edu; phone 1 404 407-8304; fax 1 404 407-7852; www.gtri.gatech.edu

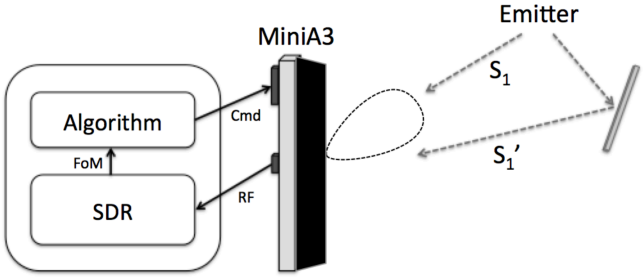

Figure 1. Illustration of the control loop formed by SDA (MiniA3) and SDR interface, enabling adaptive control of physical layer parameters: frequency, pattern, and polarization.

2. MONOLITHIC MICRODIVERSITY

The reconfigurable antenna of this study is similar to a phased array because it can form beams using an aperture. However, it is distinctly different from a phased array in that all functions, e.g. phasing, weighted combining, and frequency selection, are realized on-aperture. We have chosen to call this *monolithic microdiversity*. The designation "monolithic" is given because a single antenna structure maps the vector field over its boundary to a single RF feed. The term, "microdiversity," is used because all of the diversity degrees of freedom are realized within the space of approximately one wavelength (1.2λ for the measurements at ~2.4 GHz that are described in this paper). The small size precludes large directive gain, but is accompanied by selectivity gain.

Aperture antennas of this type can act as reconfigurable filters, tuning a response to a desired frequency, bandwidth, polarization, angle, and phase (far field). The degree of tunability in these characteristics varies and can be frequency dependent. GTRI's reconfigurable aperture work began with fragmented apertures, i.e. computer optimized pixelated antennas, reported as early as 2000 [5]. During the past 15 years, GTRI has developed L- and S-band agile aperture antennas (A3s) using commercial RF switches. These antennas use a switch matrix to variably interconnect electrically small metal segments on an aperture [6-7]. This allows somewhat arbitrary current control over the radiating surface. Both models and measurements show that, for a single-feed aperture, greater switch density is necessary to approach aperture limit gain at higher frequencies [8-10]. Because achieving efficient antennas with high switch density is a challenge in itself, work is also underway to explore the utility of such antennas in situations in which reconfigurability could be more important than absolute gain, e.g. channel selection.

This paper investigates channel selectivity for a 6x6x1 inch reconfigurable aperture antenna having 98 reconfigurable elements (unit cells) with 4 switches (bits) each. The antenna has a single RF feed point (SMA connector) and control connections (power, USB, RS-232, and IMU). The DC control power requirement is less than 125 mW but can vary depending upon configuration, peripherals, etc. The internal controller can communicate with an external inertial measurement unit (IMU) to point beams automatically. In this work, the inertial sensor feature is not used. Instead, the antenna state library and optimization technique are studied. Fig. 2 shows an example beam map and the radiation direction is defined as "into the page," a convention that is also used in Fig. 6. Selected pointing directions in the azimuth plane are indicated by enlarged dots and extra arrows in the azimuth plane.

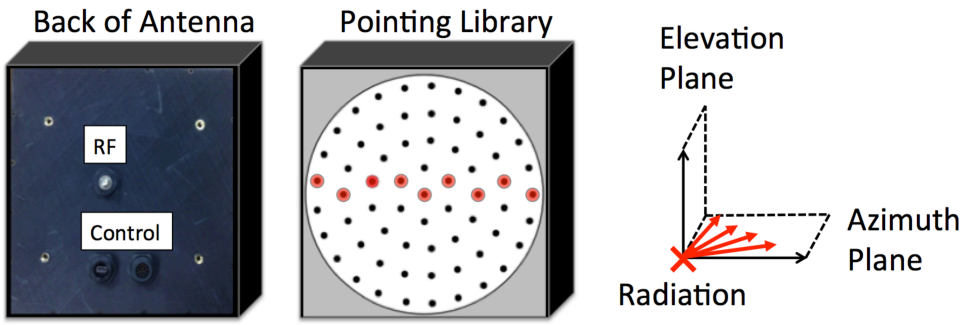

Figure 2. Diagrams looking through the back of the six-inch antenna, highlighting discrete beam states in or near the azimuthal plane of a 120° cone.

2.1 Antenna Characteristics

The six-inch reconfigurable aperture antenna is evaluated for versatility in channel selection; the absolute gain, impedance match, antenna pattern, and instantaneous bandwidth are not important. However, some of that data is provided in this section to illustrate the frequency reconfigurability of the antenna and the possibility of channel selection studies in other frequency bands. The frequency tuning performance envelope of a particular antenna is shown in Fig. 3. The results show broad tuning capability between 2 and 5 GHz.

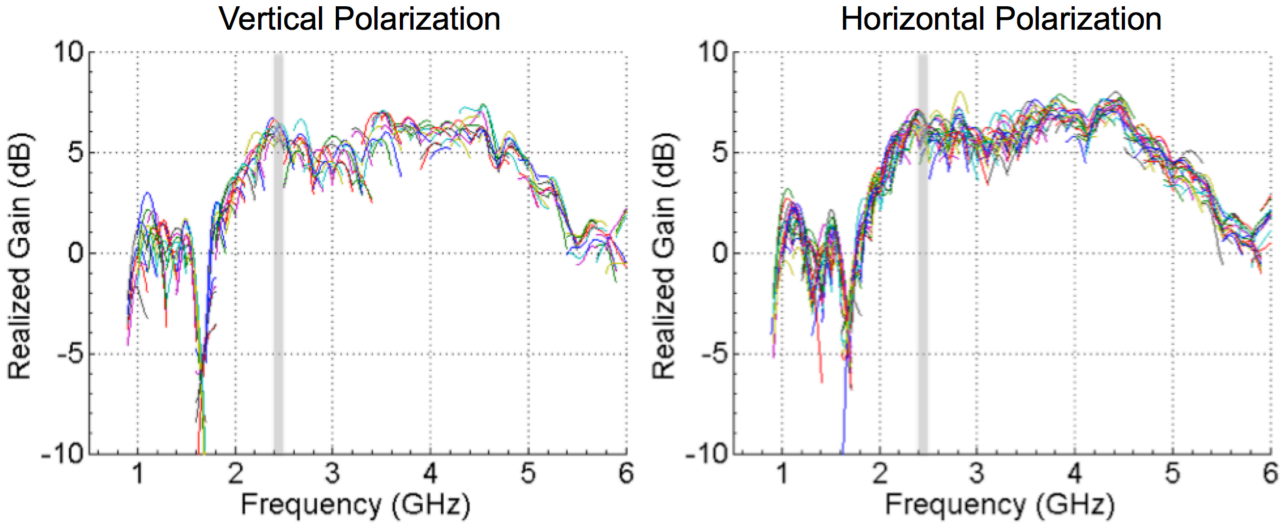

Figure 3. Frequency tuning performance of a six-inch antenna, overlaying separately optimized antenna states, each 100 MHz wide, and at 0 degrees incidence (with respect to surface normal). The frequency region of study is indicated by the vertical band.

Although this work uses the reconfigurable antenna to receive signals, the channel selection results are reciprocal, because scattering parameter measurements have shown the antenna to be reciprocal. To illustrate the applicability of the antenna to transmit mode and full duplex channels, the antenna reflection coefficient is shown in Fig. 4. The upper bound of the match of this antenna is largely determined by the feed geometry, and it is not the same for all reconfigurable antennas of this form factor. The reconfigurable lower bounds are due to changes in state that affect both radiation and losses.

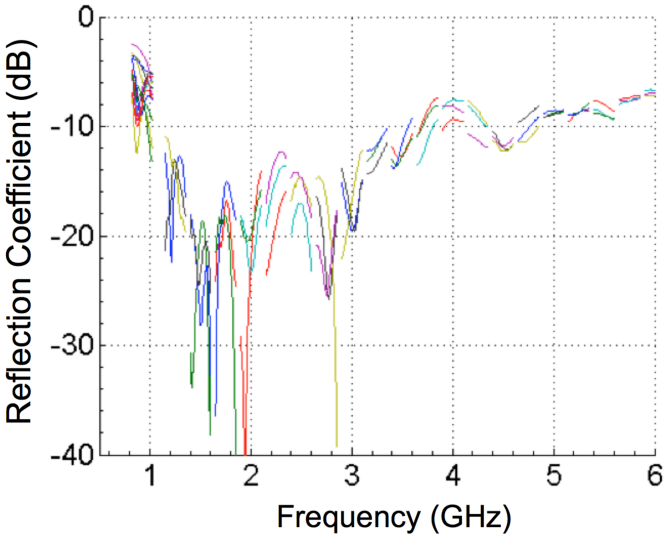

Figure 4. Overlay of reflection coefficient for states optimized for broadside gain with 100 MHz instantaneous bandwidth each.

Example radiation patterns for azimuthal pointing in two different polarizations are shown in Fig. 5. Each pattern corresponds to an optimization of gain for the same frequency band (2.4 to 2.5 GHz). The pattern diversity is evident in the peaks of the beams spanning approximately 100 degrees. Deviation from cosine scan loss is attributed to several factors: the thickness of the antenna, the internal feed arrangement, and the finite (six inch square) ground plane. Pattern symmetry and peak location were not optimization constraints and optimizations were not run to convergence; instead a fixed number of iterations was run for convenience and speed.

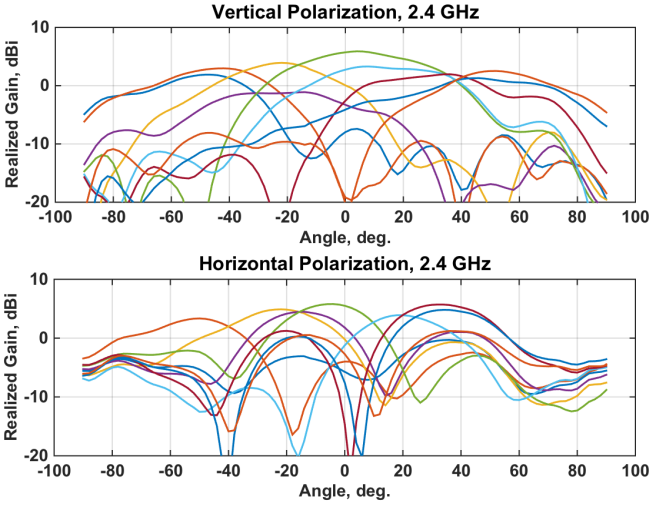

Figure 5. Patterns corresponding to optimized gain at each of 9 azimuthal directions (-60° to 60°) in two polarizations at GHz.

2.2 State Library

An antenna state library was created for evaluation of optimized states. A vector network analyzer and an illuminating antenna having a desired polarization were used with a GA to optimize the gain at many different angles. Through an iterative procedure, a 60 degree half-angle field of view was optimized, with angles sampled approximately every 15 degrees in both azimuth and elevation. Fig. 6 shows peak optimized gains at each pointing angle in one quadrant, out to 60 degrees of scan.

The same optimization procedure was repeated for horizontal, right-hand circular, and left-hand circular polarizations, producing a state library containing all 4 polarizations at several different frequencies and scan angles. In this work, the state library is limited to the pattern and polarization states lying in the azimuth plane and optimized for gain between 2.4 and 2.5 GHz. Therefore, knowing the operating frequency reduces the library size and search time (over 5 GHz tuning range sampled in 100 MHz steps) by a factor of about 50.

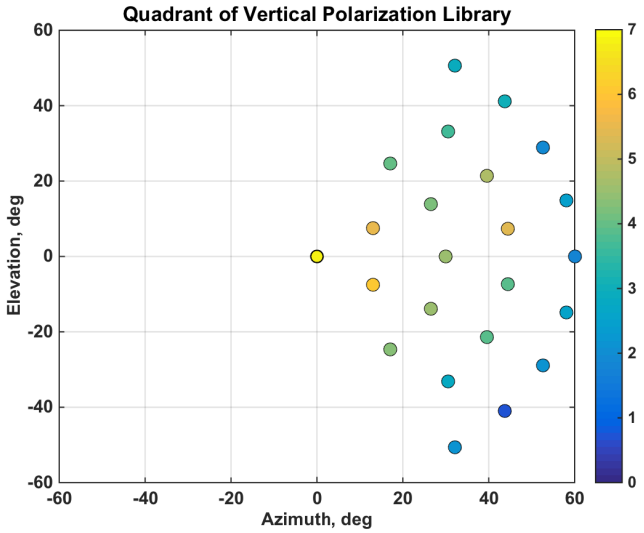

Figure 6. Peak gains of 23 optimized beams in a single quadrant (2.5 GHz library).

3. EXPERIMENT

3.1 Setup

A compact range was used for testing operation of software radios with software antennas (A3). For this experiment the reflector and much of the pyramidal absorber were left in place, but the test equipment was placed away from the focus of the reflector. Because there are line of sight paths between the transmitters (S1 and S2 in Fig. 7) and the receive antenna, Rician fading channels are expected; the exact geometry of the environment is not important. The goal of this work is to evaluate antenna reconfigurability for automatic improvement of link performance through different propagation channels.

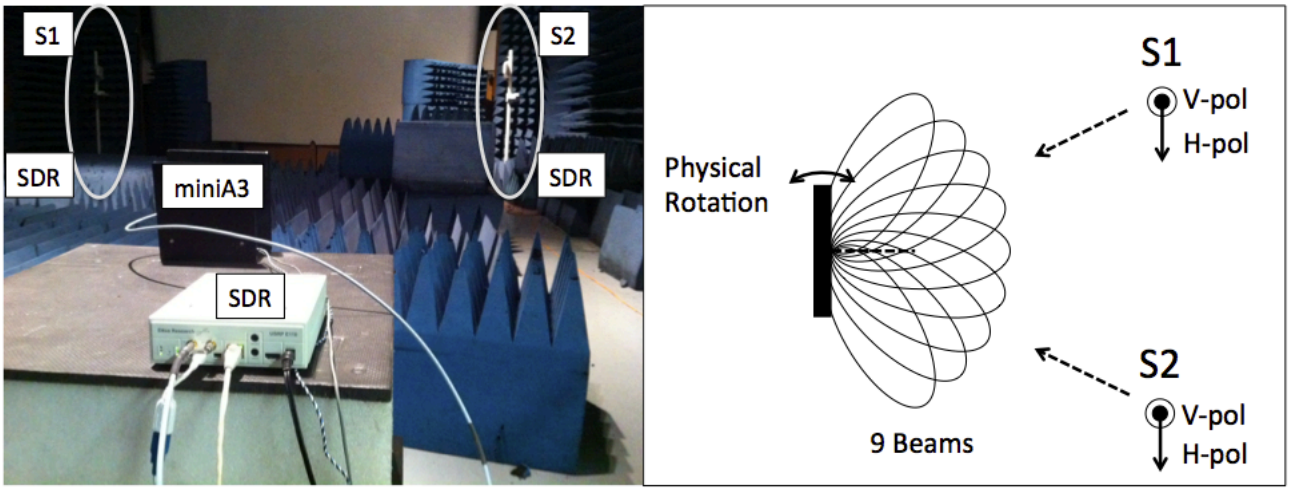

(a) (b)

Figure 7. Photograph (a) and plan view diagram (b) of the experimental setup.

3.2 Antennas

The transmit antennas at nodes "S1" and "S2" were broadband log periodic dipole arrays, Wilson 304411 oriented in vertical polarization and Antenna Factor DB1-LP oriented in horizontal polarization on 3-inch PVC masts approximately 10 meters from the receiver. The antennas were rated to produce approximately 9 dBi gain at 2.5 GHz. Each transmit antenna was provided unobstructed line of sight to the receive antenna, ensuring a Rician fading channel.

3.3 Radios

The three software radios used in this study were all from the Ettus Research product line. The two transmitters, "S1" and "S2," were E310 units having two different transmit ports. One port of each radio was connected to a vertically polarized antenna, and the other to a horizontally polarized antenna. All radios were configured with 1 MHz sample rate and the transmit radios produced approximately -40 dBm output power at the external connectors. Because radios also include embedded linux operating systems, a custom gnuradio flow graph and python TCP/IP server were designed to enable automatic evaluation of antenna states under different conditions.

3.4 Repeatability

In baseline characterizations of the experimental setup, a series of measurements were collected to verify repeatability and determine the minimum conclusive improvement in the channel. The standard deviation of received power was 0.037 dB, and the spread of the mean across several repeated tests was 0.25 dB. This indicates that the detection limit for channel fluctuations is approximately 0.5 dB with this setup. Fig. 8 shows repeated measurements of a constant beam state that boosted the relative received power by about 6.4 dB; the limit of detection was derived from these data.

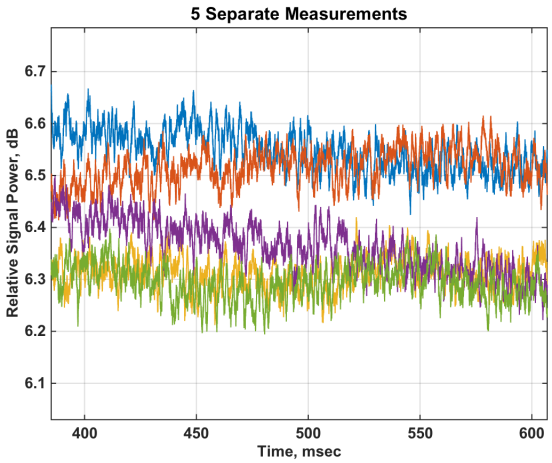

Figure 8. Variation of received power during a 0.2 second interval in which the aperture state is constant. The data correspond to five repetitions of a five-second measurement.

The consistency of the measurement is also evident at larger time and amplitude scales, e.g. through antenna state transitions. The close agreement of seven overlaid measurements of Fig. 9 confirm the repeatability of the measurement technique, the consistency of the aperture update code, and the stability of the radio transmit and receive power in the described test environment. The changes in received power are significant: more than 6 dB between steady states, and excursions of several decibels while the aperture is in transition. Although the aperture need not be updated incrementally in this way, this measurement highlights the fact that intermediate effective fades can be present during a transition. These changes and their corresponding time scales are discussed in the following section.

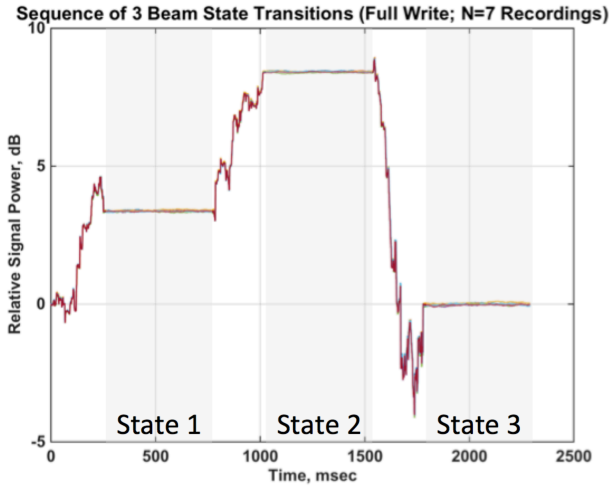

Figure 9. Measurement of baseband received signal power through antenna state transitions.

3.5 Autofading

We use the term, "autofade," to refer to the apparent variation of the propagation channel due to deliberate change of antenna state. This phenomenon occurs during adaptation of a reconfigurable antenna, and this paper investigates the severity of the fades through different state changes. The objective is to minimize such fades during link adaptation. Indeed, if the optimization process degrades the channel too severely, the short-term penalty may not be worth the long-term gain.

Autofade in reconfigurable antennas having discrete digital switches can be divided into at least two components, as shown in Fig. 10. The first is the fast component, corresponding to the transition time of the antenna. This is the time interval during which the switches change state and the RF performance differs from both the previous state and the next state. The second component is slower and is due to the differences between two states.

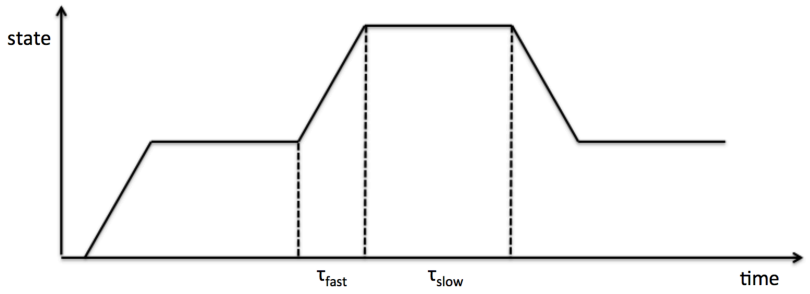

Figure 10. Illustration of antenna state transitions and autofade components.

During adaptation, the radio causes the antenna to remain at each state long enough to determine the quality of the link. If the antenna realizes a state of worse performance during adaptation, the corresponding autofade will exist for at least the integration time necessary to assess link performance. Therefore it is desirable for the integration time and FoM computation time to be less than the fastest autofade component. For a given integration time, a higher information rate could yield a more reliable figure of merit.

Using the Shannon channel capacity formula and assuming a signal-to-noise ratio (SNR) much greater than 1, the total information available in a given integration time is proportional to the signal bandwidth, as shown in Eq. 1, wherein B is the bandwidth (constant) and SNR is the signal-to-noise ratio as a function of antenna state, a, which varies as some function of time, t. The signal and noise power may be independent functions of antenna state.

$$C = B \log_2(1 + SNR(a(t))) \tag{1}$$

Differentiating Eq. 1 with respect to time reveals diminishing increase in the capacity, and therefore convergence rate, with increasing SNR as shown in Eq. 2.

$$\frac{\partial C}{\partial t} = \frac{B}{\ln(2)} \frac{1}{1+SNR(a(t))} \frac{\partial}{\partial t} SNR(a(t)) \quad (2)$$

At low SNR, an improvement in antenna state will yield greater increase of the capacity. Also, while greater channel bandwidth implies greater capacity and faster convergence, it also implies greater impact of a given autofade to a communications channel: more bits are lost in the same unit of time.

It was expected that knowledge of link parameters could reduce the negative impacts of autofade by eliminating states certain to have poor performance, e.g. wrong frequency. We evaluated this possibility by using a library of antenna states matching the expected operating conditions, i.e. ~2.4 GHz and pointing only in the horizontal (azimuthal) plane. The next section reports the use of small libraries (N_i=9 or N_i=36 states) having diversity in pattern and/or polarization at one frequency band.

4. LIBRARY EXPERIMENTS

In the following library experiments, two separate transmitters challenged the antenna in selecting channels at different angles and polarizations, and with different receive antenna orientations. Because all radios had the same local oscillator frequency, the two emitters were distinguished in baseband by simple tones, similar to the continuous tone-coded squelch system (CTCSS). Fig. 11 shows the two tones that were present in 144 overlaid measurements and with sufficient dynamic range to observe fluctuations in received power due to changes in the propagation channel or the antenna state. The power in the frequency bins corresponding to the two transmitters, "S1" and "S2," was sampled and used in computing a channel figure of merit (FoM).

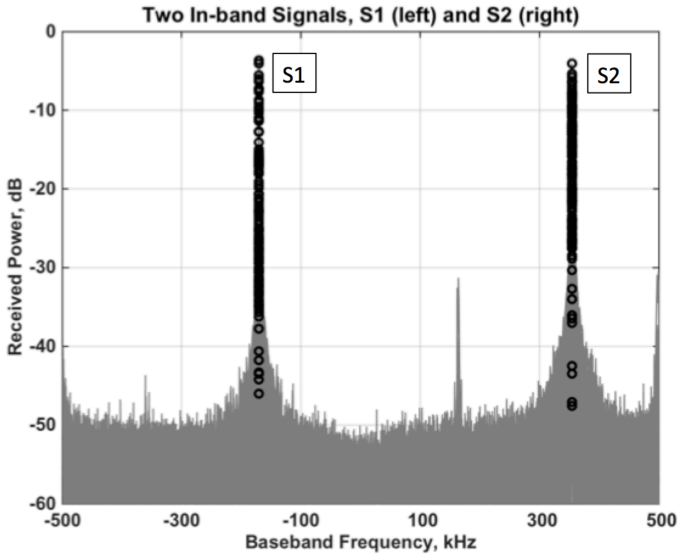

Figure 11. Frequency spectrum of baseband samples at 1 MHz sample rate for 144 overlaid measurements corresponding to 36 receive antenna states and 2 transmit polarizations at each of 2 transmitters. Open circles indicate power data selected for further analysis.

4.1 Pattern Channel Selection

This first experiment used a small library of nine beams in the azimuthal plane and having vertical polarization. The nine beams are highlighted in Fig. 2. In the following measurements, complex baseband power spectrum was post-processed to evaluate channel selection by way of the baseband tones shown in Fig. 11. A FoM was devised as the ratio of power from S1 (denoted P1) and power from S2 (denoted P2), in order to select S1 in preference to S2. That FoM is plotted for five antenna orientations (vertical axis) and nine antenna beam states (horizontal axis) in Fig. 12. To evaluate the ability of the antenna to provide improved performance at every attempted orientation, inspection of the rows shows at least one positive FoM in every row (orientation), even though the average across all rows is -2 dB. This average difference is attributed to slightly different cable losses and path lengths for S1 and S2 relative to the receive antenna.

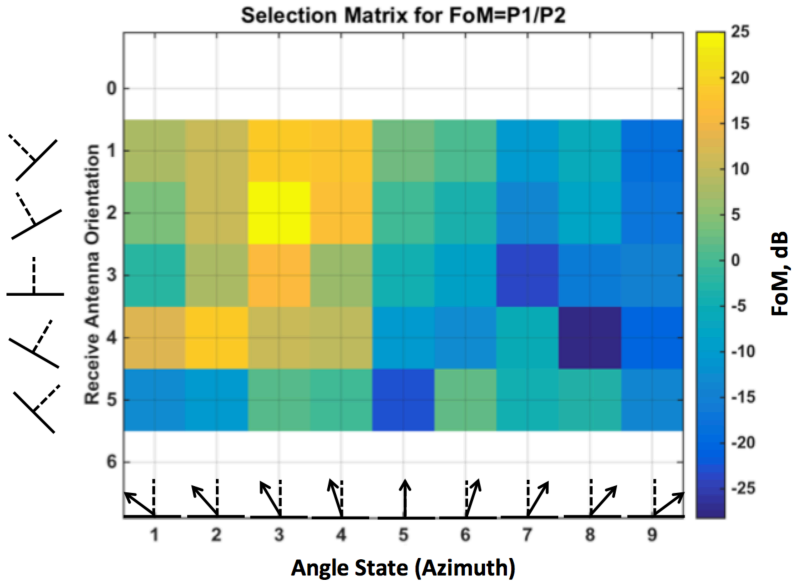

Figure 12. Channel selection matrix for power ratio figure of merit (FoM), all antennas in vertical polarization. The series of beam states is azimuthal variation of pattern up to 60 degrees from normal incidence (0 degrees is state 5).

4.2 Polarization and Pattern Channel Selection

In a second experiment, polarization was also varied. A library of four times the size was applied, having polarization diversity (V,H,L,R) for each state of the previous pattern library (9 azimuthal states). In this case, performance was evaluated for a single orientation of the receive antenna. Sixteen different configurations were evaluated, corresponding to each combination of receive polarization (V,H,L,R) at the receive antenna and transmit polarization (V,H) at each of two transmit antennas. The corresponding channel selection matrix is shown in Fig. 13.

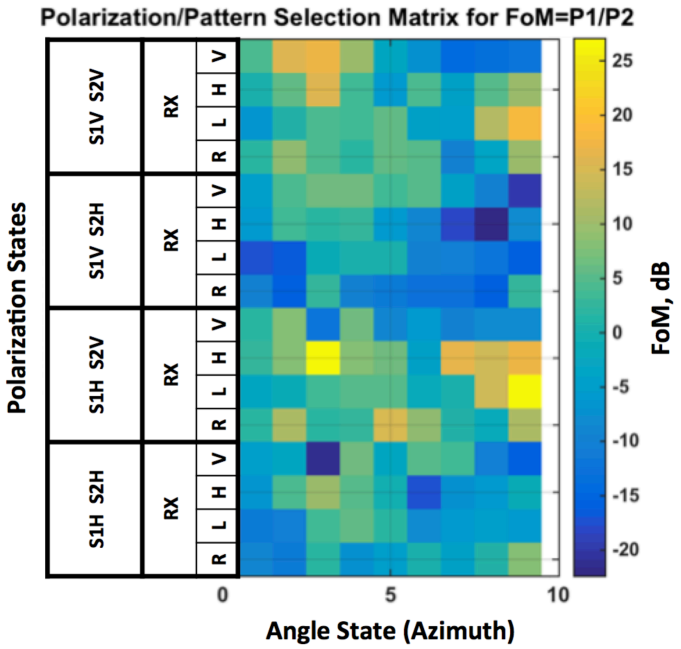

Figure 13. Channel selection matrix for power ratio figure of merit (FoM), with transmit antennas (S1, S2) and receive antenna (RX) in varied polarization states.

The minimum dynamic range across pattern states (rows) was 17 dB, and the maximum was 32 dB. This indicates that the library, composed of states optimized independently for gain at different polarizations and pointing directions, provides increased diversity but not compounded selectivity. Compounded selectivity would expand the total range of the FoM. The data also hints at nonuniform axial ratio as some linear polarizations are favored at steer despite using an aperture state optimized for circular polarization. This makes sense, given a tendency of the aperture toward linear polarization at steep angles of incidence, despite optimization for circular polarization. The expanded library remains suboptimal, as expected. The next section details optimal selection of physical channels, within the constraints of the antenna degrees of freedom.

4.3 Arbitrary Channel Selection

This section reports the *in situ* optimization and time evolution of antenna state using a genetic algorithm (GA). Genetic algorithms have been used in the design of static antennas [5] and reconfigurable antennas [7] for more than a decade. This paper reports the use of the GA to find globally optimum antenna states during radio operation, using figures of merit calculated from baseband samples. It was expected that the feedback loop and global search algorithm would achieve better performance than the library search, at the expense of greater time.

An experiment was conducted to examine convergence under various figures of merit and antenna orientations. The baseband data was processed by a gnuradio script implementing a real time FFT over 128 bins and using a Blackman-Harris window. The baseband power spectrum was continually updated and the GA sampled that spectrum as needed to compute a figure of merit for each evaluated antenna state. The computed figures of merit for optimization were power ratios: various permutations of signal-to-noise or signal-to-signal ratio. For example, optimal selection of power

from S2 is designated P2, and optimal selection of power from S1 relative to S2 is designated P1/P2. We note that the antenna and algorithm were not given any information about the physical channel; the frequency, polarization, plane of incidence, etc. were unknown to the optimizer. Furthermore, optimization began with a random antenna state.

The genetic algorithm was configured with a population size of 32, and each individual evaluation required approximately 380 milliseconds, including aperture update and calculation of the figure of merit. Therefore each generation required approximately 12 seconds to complete. Fig. 14 shows the cumulative maximum performance for four different figures of merit at each of three different antenna orientations (Left, Middle, Right) or (-30°, 0°, +30°) respectively.

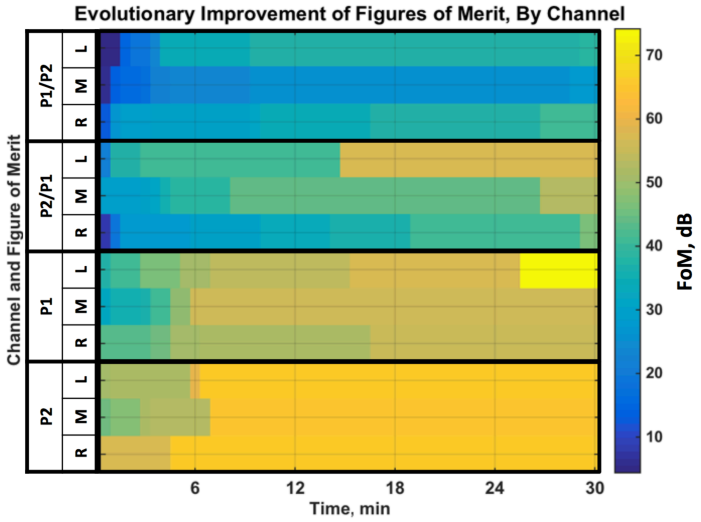

Figure 14. Plot of the cumulative maximum figure of merit (color) versus time, figure of merit, and antenna orientation. The vertical axis designates FoM (P2, P1, P2/P1, P1/P2) and orientation (L=-60°, M=0°, R=+60°).

To view the typical bounds of performance, three data series were calculated corresponding to the minimum, average, and maximum figure of merit across all trials at each point in time. For each FoM, a different initial value was observed; therefore each data series was normalized relative to the average of its first several values. Finally, a moving average was applied to indicate the short-term channel variation a radio would experience. The resulting data are shown in Fig. 15, in which the average improvement from the starting point is about 10 dB over 10 minutes, corresponding to evaluation of approximately 1600 antenna states out of 2^{392} possible for this antenna.

The average worst-case performance improves approximately 10 dB, which is an important consideration for the use of a global search technique during active communications; the impact of severe autofades decreases during adaptation. After 10 minutes, the spread between the average FoM and the high-performing outliers, the goal of the evolutionary search, is an additional 10 dB beyond the average starting point.

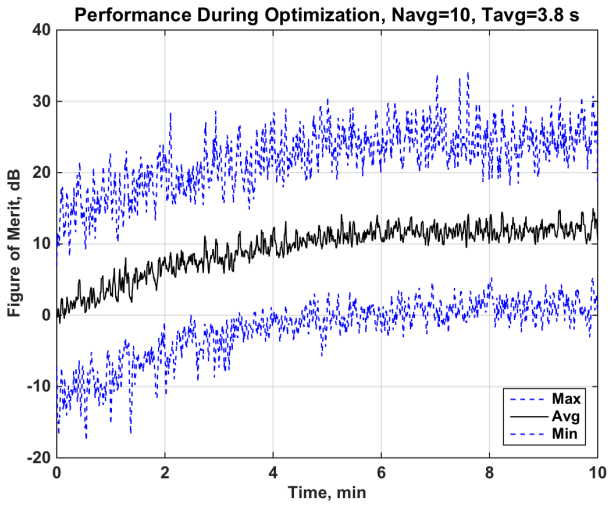

Figure 15. Moving average performance during optimization, across twelve different trials including four different figures of merit and three antenna orientations.

5. DISCUSSION

Signal fading is often addressed using MIMO techniques. In this work, the library technique is most like selection diversity, in which the antenna state and corresponding channel with the greatest figure of merit is selected. In high SNR environments this is expected to be useful because a library can be provided that maximizes diversity, i.e. the independence of the antenna states. The evolutionary technique is more similar to maximal ratio combining because the aperture can evolve to a state that is effectively a combination of library states, achieving a better result in a given environment than any individual library state. In low SNR environments this is expected to be useful because an optimal state is required to close the link.

In this work Rayleigh fading was not addressed, and both static shadowing and fast fades remain to be investigated. In such conditions, no adjustment to the antenna state can provide a Rician fading diversity branch, but a usable and potentially optimum Rayleigh fading diversity branch may be available within the large number of possible antenna states. There are at least two challenges in this case: finding the optimum state fast enough, and providing this degree of reconfigurability with high enough antenna efficiency.

An advantage of the monolithic microdiversity enabled by a reconfigurable antenna is that it could be applied to every available radio port in a system. Existing diversity techniques range from single-feed, connecting a few switched static antennas to a single radio, to true MIMO systems having several antennas and several radios for optimal combining [11]. For a fixed number of transceivers in a given MIMO system, reconfigurable antennas such as the type described in this paper could be used to provide optimal MIMO, an approach already described in the literature [12].

In MIMO problems there are two key operating regimes that deserve discussion: low SNR and high SNR. It is possible that reconfigurable antennas soon will improve MIMO in both regimes. At low SNR, an optimized antenna state could be optimized N times more rapidly, performing optimization at each of N available radio channels simultaneously. The best solution then could be applied to all N antennas at once. This would be equivalent to maximizing an eigenvalue of the channel matrix,

and then duplicating it across N radio channels. At high SNR, as in the experiments of this paper, the condition number of the channel matrix could be maximized, meaning each antenna could be optimized to a different state with high gain.

6. CONCLUSIONS

A six-inch square Agile Aperture Antenna (A3) was evaluated for channel selection in unknown or uncharacterized environments. A network of software defined radio transceivers was used to illuminate the reconfigurable antenna at differing angles and polarizations. The experimental setup and the antenna were evaluated for consistency throughout repeated measurements. Using relatively small antenna state libraries (N_i=9 and N_i=36), channel selection matrices were shown to assess the ability of the antenna to mitigate multipath fades in future applications. Using a genetic algorithm and real time measurement of the baseband power spectrum, several different figures of merit were computed to identify the transmitters. All figures of merit showed improvement, although at different rates and degrees. Average performance bounds were presented for the optimizations, revealing an average improvement of 10 dB, and additional 10 dB of best-performing outliers. The authors expect that the A3 and the computer automated test environment described in this paper can be used to examine dynamic channels.

7. ACKNOWLEDGEMENTS

The authors would like to thank Gregory Kiesel and William Hunter for development of the Agile Aperture Antenna (A3), and Charlie Hunter and Cameron Phillips for antenna measurements and diagnostics.

This effort was supported in part by GTRI internal research and development funds, allocated under the Spectrum Strategic Initiative led by Eric Barnhart of the Information and Communications Laboratory (ICL).

8. REFERENCES

[1] Seidel, S. Y., & Rappaport, T. S. (1994). Site-specific propagation prediction for wireless in-building personal communication system design. IEEE Transactions on Vehicular Technology, 43(4), 879–891.

[2] Gesbert, D., Bolcskei, H., Gore, D.A., & Paulraj, A.J. (2002). Outdoor MIMO wireless channels: models and performance prediction. IEEE Transactions on Communications, 50(12), 1926–1934.

[3] Forenza, a., Pandharipande, A., Hojin Kim, & Heath Jr., R. W. (2005). Adaptive MIMO Transmission Scheme: Exploiting the Spatial Selectivity of Wireless Channels. In 2005 IEEE 61st Vehicular Technology Conference (Vol. 5, pp. 3188–3192).

[4] Bernhard, J. T. (2003). Reconfigurable Antennas and Apertures: State-of-the-Art and Future Outlook, 5055, 1–9.

[5] Maloney, J. C., Kesler, M. P., Lust, L. M., Pringle, L. N., Fountain, T. L., Harms, P. H., & Smith, G. S. (2000). Switched fragmented aperture antennas. In IEEE Antennas and Propagation Society International Symposium. Transmitting Waves of Progress to the Next Millennium. 2000 Digest. Held in conjunction with: USNC/URSI National Radio Science Meeting (Cat. No.00CH37118) (Vol. 1, pp. 310–313).

[6] Pringle, L. N., Harms, P. H., Blalock, S. P., Kiesel, G. N., Kuster, E. J., Friederich, P. G., … Smith, G. S. (2003). The GTRI prototype reconfigurable aperture antenna. In IEEE Antennas and Propagation Society International Symposium. Digest. Held in conjunction with: USNC/CNC/URSI North American Radio Sci. Meeting (Cat. No.03CH37450) (Vol. 2, pp. 683–686).

[7] Pringle, L. N., Harms, P. H., Blalock, S. P., Kiesel, G. N., Kuster, E. J., Friederich, P. G., Smith, G. S. (2004). A Reconfigurable Aperture Antenna Based on Switched Links Between Electrically Small Metallic Patches. IEEE Transactions on Antennas and Propagation, 52(6), 1434–1445.

[8] Mehmood, R., & Wallace, J. W. (2010). Diminishing Returns With Increasing Complexity in Reconfigurable Aperture Antennas. IEEE Antennas and Wireless Propagation Letters, 9, 299–302.

[9] Kiesel, G.N., and Cook, K.R. (2015). Optimization of Pixelated Antennas. In IEEE International Symposium on Antennas and Propagation.

[10] Westafer, R. S., Morris, A. P., & Lee, R. T. (2015). A reconfigurable electromagnetic interface to ease requirements on phased array common modules. In SPIE 9479, Open Architecture/Open Business Model Net-Centric Systems and Defense Transformation 2015, 947904, R. Suresh (Ed.).

[11] Oswald, M. T., Hagness, S. C., Van Veen, B. D., & Popovic, Z. (1999). Reconfigurable single-feed antennas for diversity wireless communications. In IEEE Antennas and Propagation Society International Symposium (IEEE Cat. No. 02CH37313) (Vol. 1, pp. 469–472). IEEE.

[12] Cetiner, B. a., Akay, E., Sengul, E., & Ayanoglu, E. (2006). A MIMO system with multifunctional reconfigurable antennas. IEEE Antennas and Wireless Propagation Letters, 5(December), 463–466.